U.S. Department of Veterans Affairs
VA Greater Los Angeles Healthcare System

Reliability of 2D-Speckle-Tracking for Myocardial Strain Measurements

Bobby Patel[1,2], Maxwell Reynolds[1,2], Kim-Lien Nguyen MD[1]
[1]Division of Cardiology, David Geffen School of Medicine at UCLA and VA Greater Los Angeles Healthcare System
[2]Department of Ecology and Evolutionary Biology, University of California, Los Angeles

Background

Myocardial strain imaging using 2D-speckle-tracking echocardiography (STE) is a relatively new method for analyzing myocardial function.[1] Myocardial strain measures the shortening of myocytes in three directions: longitudinally, circumferentially, and radially. While ejection fraction (EF) is a common measure of heart health, strain measurements are more sensitive to changes in ventricular function and thus can be used to detect subclinical cardiac abnormalities that may not be seen by EF measurements.[2] Strain values for various chambers have implications for identifying and treating many different cardiomyopathies.[2,4-5] Speckle-tracking echocardiography and tissue Doppler imaging (TDI) are the two primary methods for measuring strain using echocardiography. STE is more clinically relevant than TDI due to its ability to distinguish passive tethering from active contractility and its independence of ultrasound beam angle.[3] Reliability of strain measurements from STE is not universally agreed upon due to vendor differences in strain analysis algorithms. LV GLS tends to consistently have the greatest reliability and thus the most significant clinical application. LV GCS and GRS, LA GLS, RA GLS, and RV GLS have more mixed results and have not been implemented as widely as LV GLS.[7-10]

Methods & Approach

Methods: STE was performed using a commercially available, 3rd party software (TomTec). A semi-automated technique with manual user adjustments was used to analyze 2-dimensional images in the apical long and parasternal short-axis views: apical 2-chamber (A2C), apical 3-chamber (A3C), apical 4-chamber (A4C), and short-axis images at the basal, mid, and apical ventricular views. Images were excluded if more than 2 segments of dropout was observed for any of the defined 2-dimensional views[12], or has poor tracking. Image quality (based on a 5 point Likert scale grading system) was done based on consensus.

Approach: Two observers analyzed 20 echocardiographic datasets. To obtain strain values, the cine-loops with the best image quality were chosen. Endocardial and epicardial borders were defined at end-systole and manual adjustments were performed at both end-diastole and end-systole (Figure 1). The values obtained from these corresponding studies were used to calculate inter-observer agreement. The time interval for intra-observer tracing was 4 months.

Table 1. Inter and Intra-observer strain reliability statistical results

Inter-observer	Coefficient of Repeatability	Mean	Upper LoA	Lower LoA	ICC	CoV (%)
LVGLS	1.79 (95% CI 1.37-2.58)	0.1	1.9	-1.7	0.94	-4.27
LVGCS	7.68 (95% CI 5.88-11.09)	2.2	8.7	-4.4	0.87	-11.62
LVGRS	20.74 (95% CI 15.87-29.95)	-7.3	8.2	-22.7	0.79	20.99
LAGLS	32.50 (95% CI 24.86-46.93)	-8.1	21.1	-37.2	0.86	11.72
RAGLS	29.29 (95% CI 22.41-42.29)	9.6	32.6	-13.4	0.74	29.93
RVGLS	8.89 (95% CI 6.81-12.84)	2.3	10.2	-5.5	0.71	-19.14

Intra-observer 1	Observer 1 ICC	Observer 1 CoV (%)
LVGLS	0.93	-4.35
LVGCS	0.97	-4.26
LVGRS	0.93	11.1
LAGLS	0.97	9.97
RAGLS	0.92	11.16
RVGLS	0.78	-12.29

Intra-observer 2	Observer 2 ICC	Observer 2 CoV (%)
LVGLS	0.95	-4.46
LVGCS	0.98	-3.9
LVGRS	0.92	11.26
LAGLS	0.93	12.46
RAGLS	0.93	13.69
RVGLS	0.84	-15.78

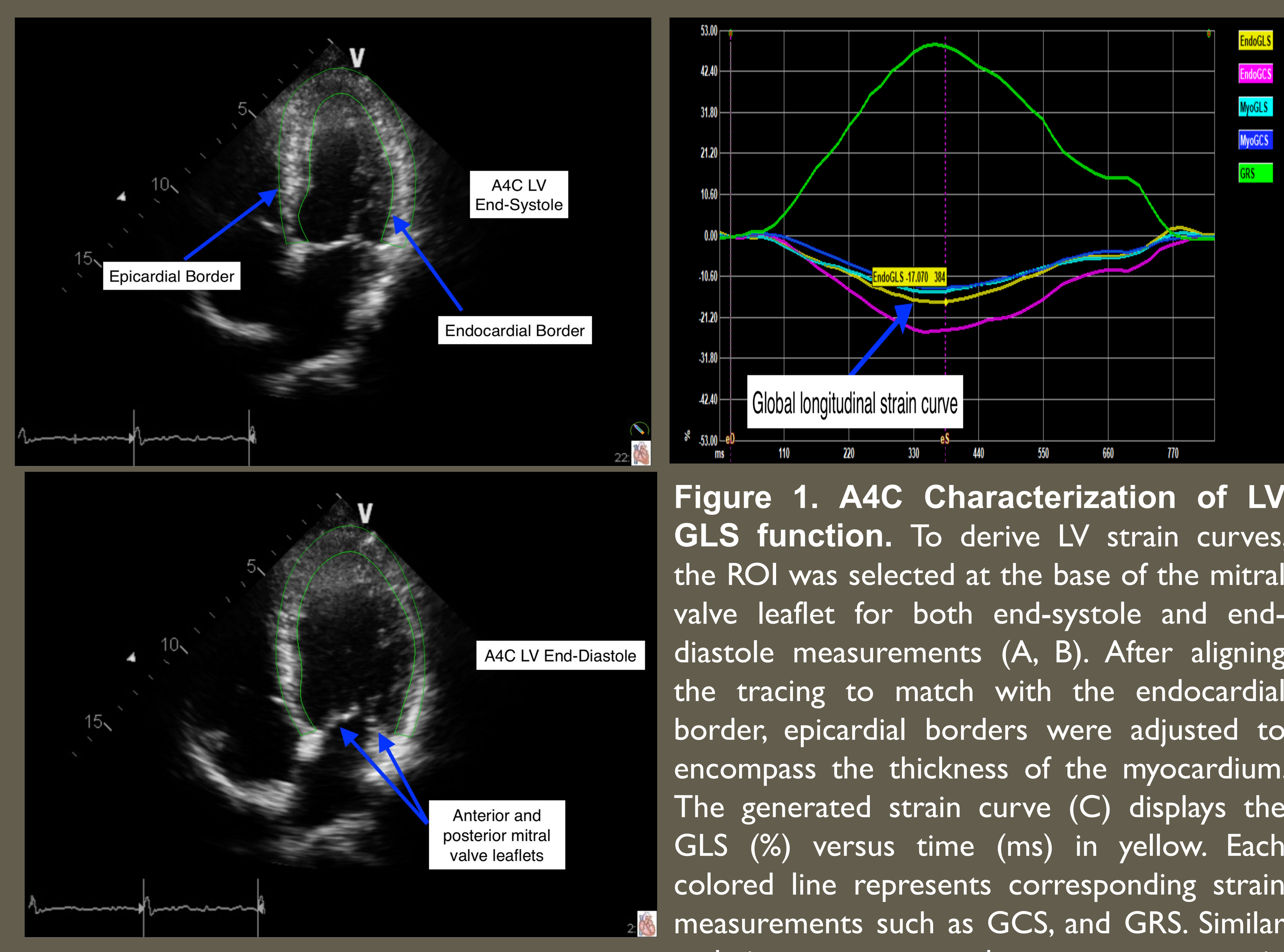

Figure 1. A4C Characterization of LV GLS function. To derive LV strain curves, the ROI was selected at the base of the mitral valve leaflet for both end-systole and end-diastole measurements (A, B). After aligning the tracing to match with the endocardial border, epicardial borders were adjusted to encompass the thickness of the myocardium. The generated strain curve (C) displays the GLS (%) versus time (ms) in yellow. Each colored line represents corresponding strain measurements such as GCS, and GRS. Similar techniques were used to generate strain curves for RA, RV, and LA chambers.

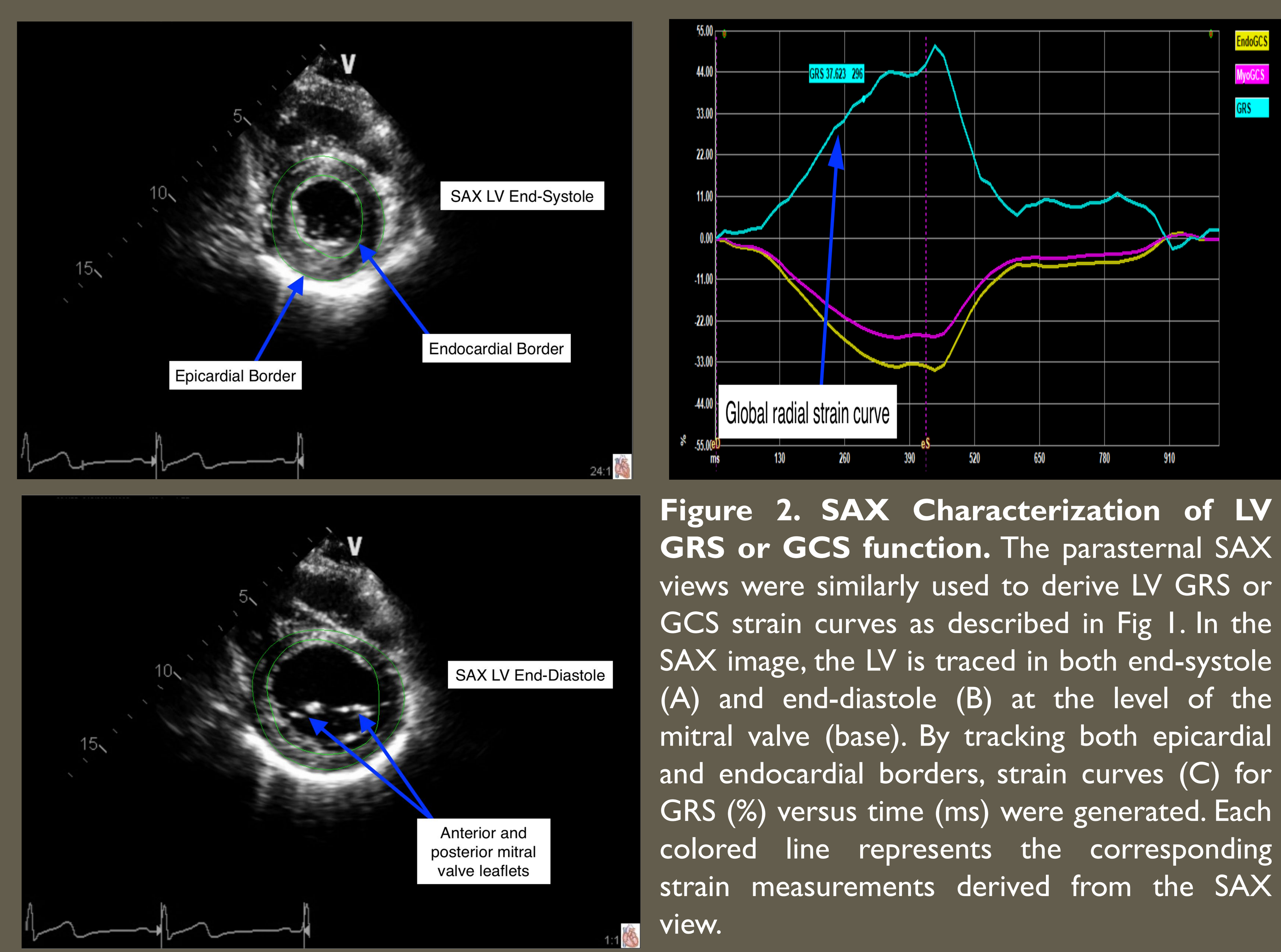

Figure 2. SAX Characterization of LV GRS or GCS function. The parasternal SAX views were similarly used to derive LV GRS or GCS strain curves as described in Fig 1. In the SAX image, the LV is traced in both end-systole (A) and end-diastole (B) at the level of the mitral valve (base). By tracking both epicardial and endocardial borders, strain curves (C) for GRS (%) versus time (ms) were generated. Each colored line represents the corresponding strain measurements derived from the SAX view.

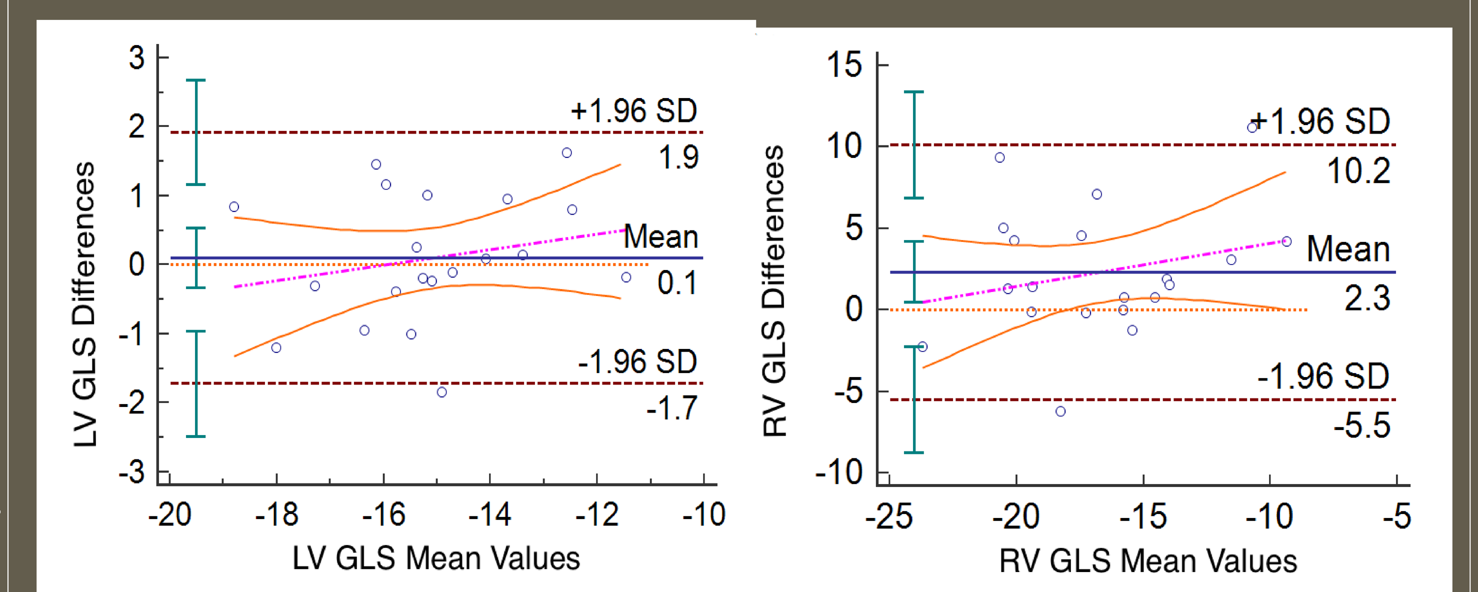

Figure 3. Bland-Altman plots for inter-observer strain measurements of LV GLS (left) and RV GLS (right). For LV GLS, the mean difference found between observers was 0.1 with the upper LoA at 1.9 and lower LoA at -1.7 (95% C.I. 1.37-2.58). For RV GLS, the mean difference found between observers was 2.3 with the upper LoA at 10.2 and lower LoA at -5.5 (95% C.I. 6.80-12.84). When comparing LV and RV GLS interobserver strain values, there is greater variability observed for RV GLS. Bland-Altman plots were additionally constructed for RV, RA, and LA chambers to display variability for GCS, GRS, and GLS. The relationship between image quality and interobserver differences was not statistically significant (p=0.82) but showed trend of higher variability with worse image quality. *LoA*, limits of agreement; *CI*, confidence interval.

Conclusions

Conclusions: Our work demonstrates excellent inter and intra-observer agreement for LV GLS and agrees well with prior published work and feasibility for application in clinical practice. LV GCS, LV GRS, and LA GLS also are promising, with good inter-observer agreement and excellent intra-observer agreement. RA and RV GLS were less reliable compared to left heart measurements. Although not statistically significant, the general positive relationship between image quality and measurement agreement suggests that poor image quality was likely a factor in inter- and intra-observer variability. When performing STE with multiple observers, consistent training practice with set procedures and guidelines will contribute to greater reliability for acquired strain measurements.

Limitations: Due to the retrospective nature of the analysis and the images being obtained for other purposes, the echocardiographic views obtained were not always optimal for strain analysis. However, all images had adequate frame rate and each set of images were analyzed for quality before inclusions.

Future Directions

Inter- and intra-observer assessment using images focused on the right heart is needed to truly measure their reliability. Although there was a relationship between poor image quality and greater variability in inter-observer strain measurements, more work is needed to determine optimization strategies for image quality. Currently, myocardial strain analysis is not performed in all clinical echocardiographic laboratories. To demonstrate the added-value of myocardial deformation analysis in the practice setting, additional work is needed to 1) determine the data processing time necessary for strain analysis and 2) devise automated strategies to minimize analysis time and to improve precision.

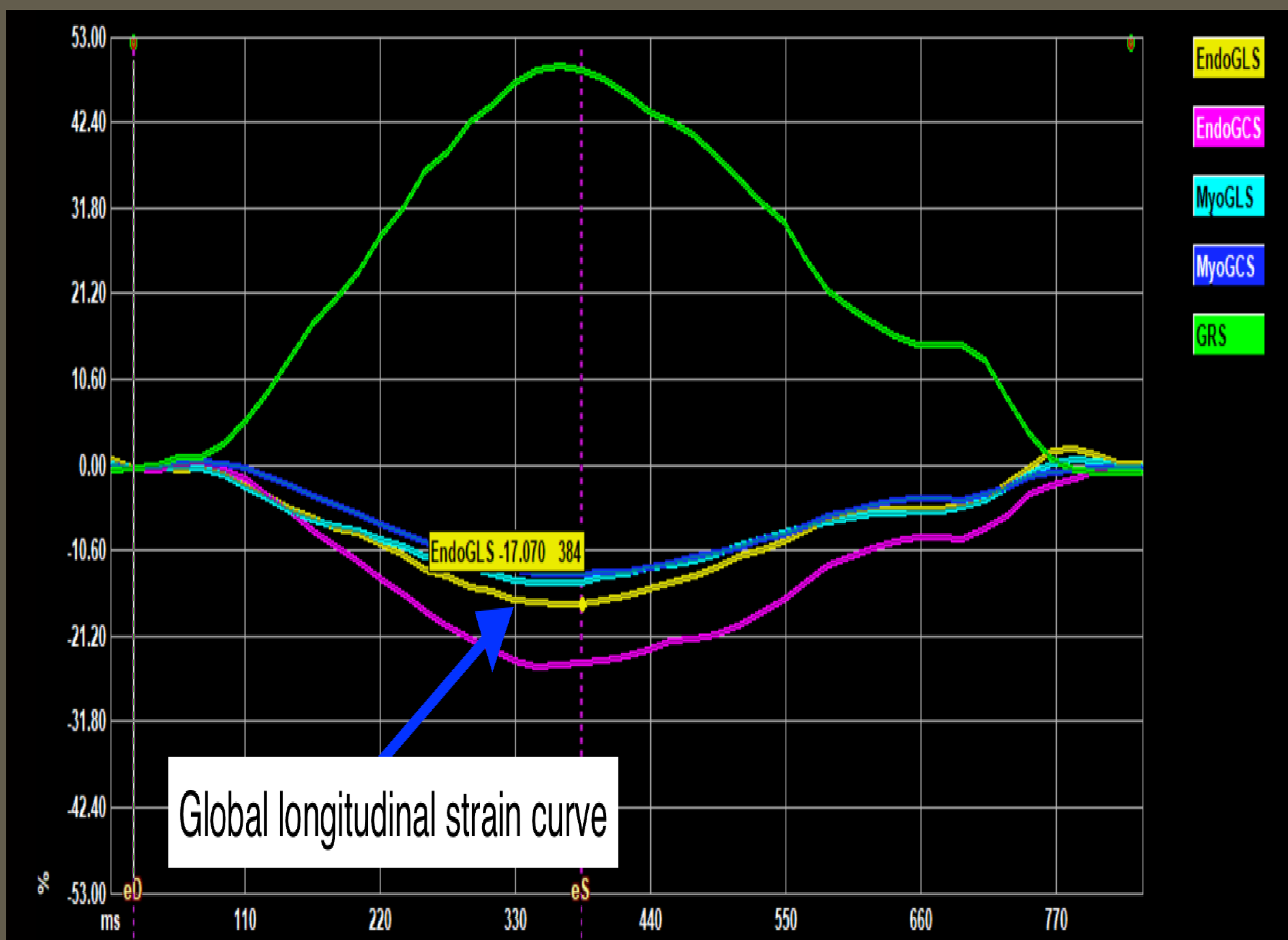

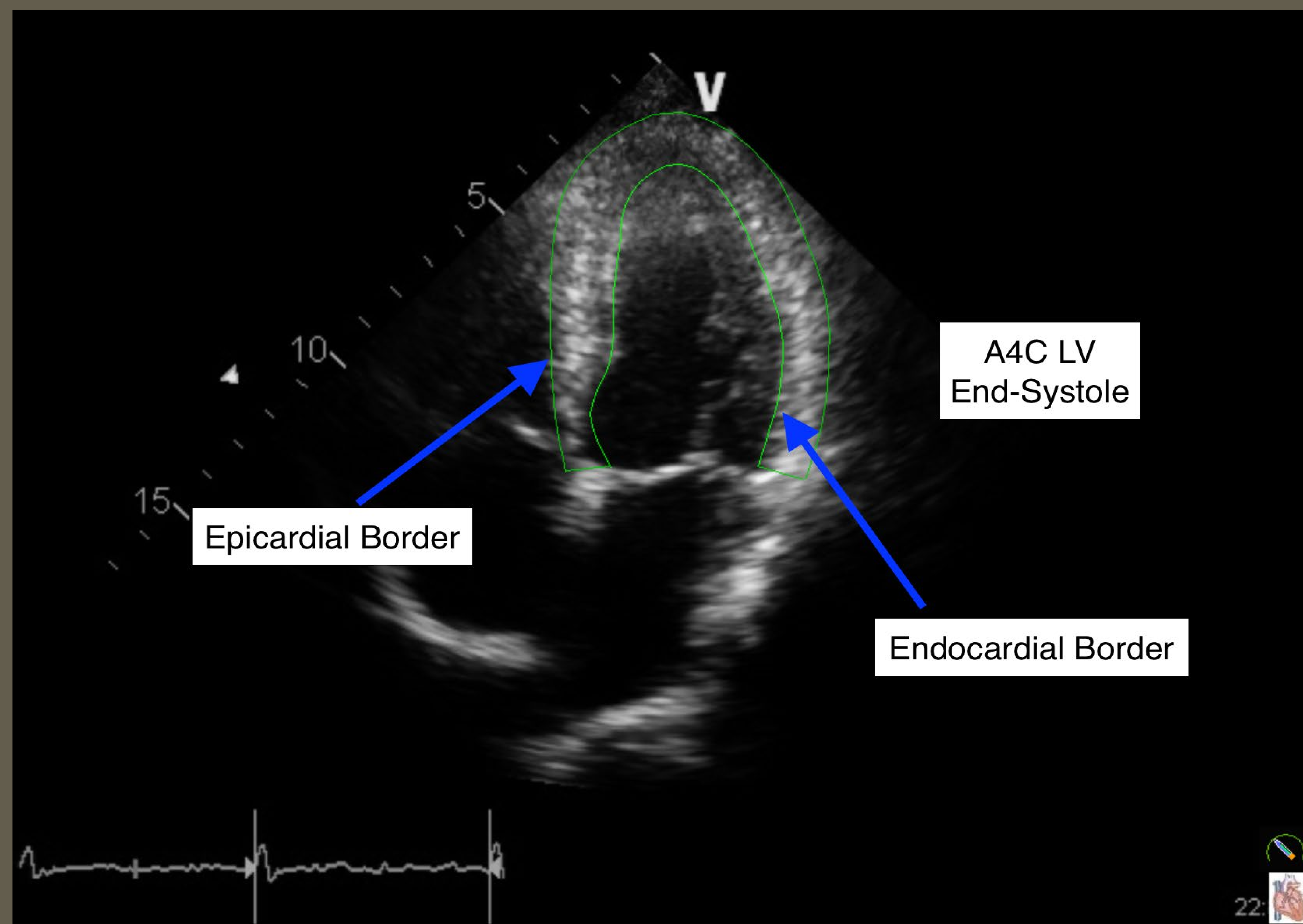

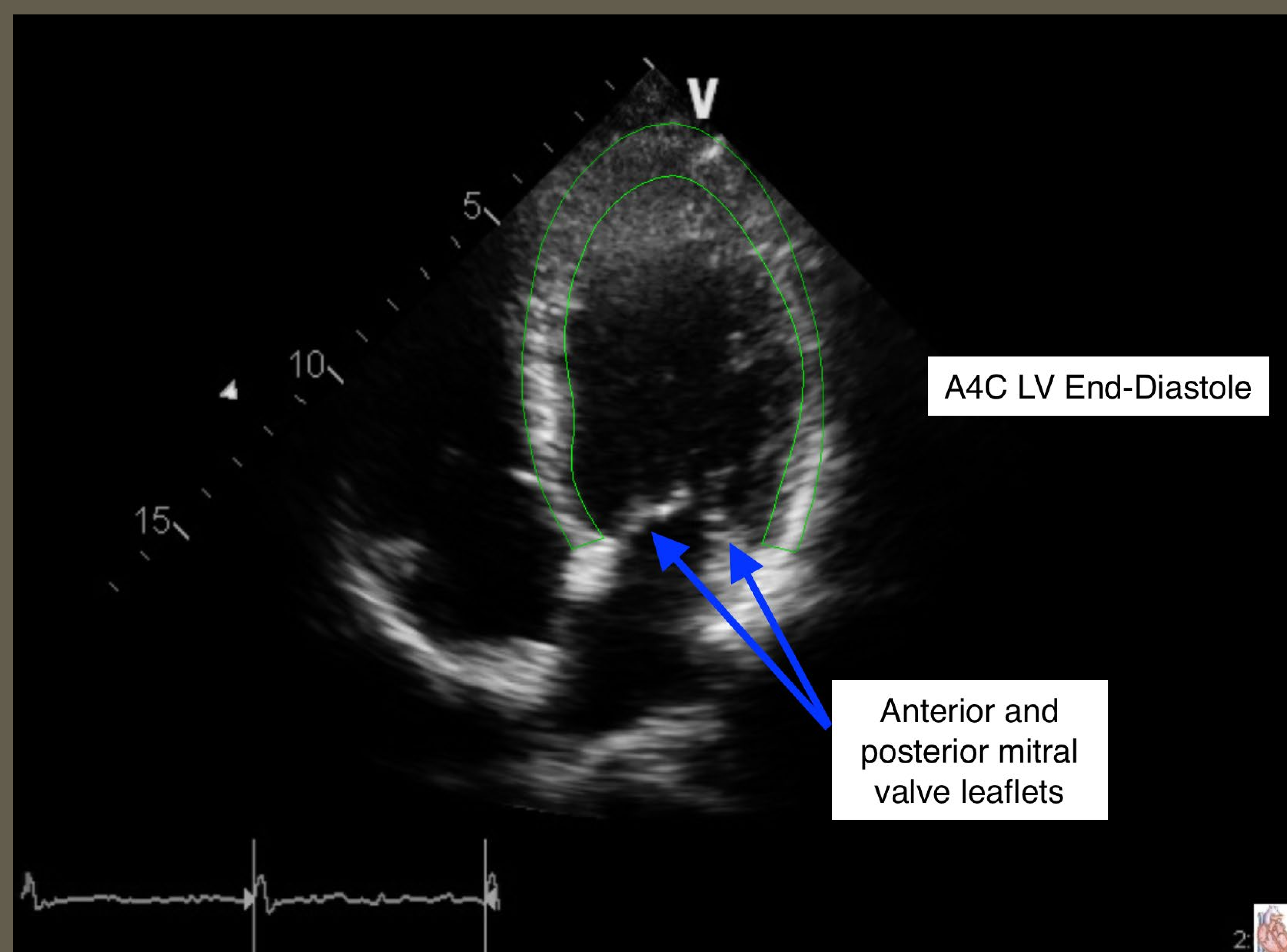

Figure 1. A4C Characterization of LV GLS function.

To derive LV strain curves, the ROI was selected at the base of the mitral valve leaflet for both end-systole and end-diastole measurements (A, B). After aligning the tracing to match with the endocardial border, epicardial borders were adjusted to encompass the thickness of the myocardium. The generated strain curve (C) displays the GLS (%) versus time (ms) in yellow. Each colored line represents corresponding strain measurements such as GCS, and GRS. Similar techniques were used to generate strain curves for RA, RV, and LA chambers.

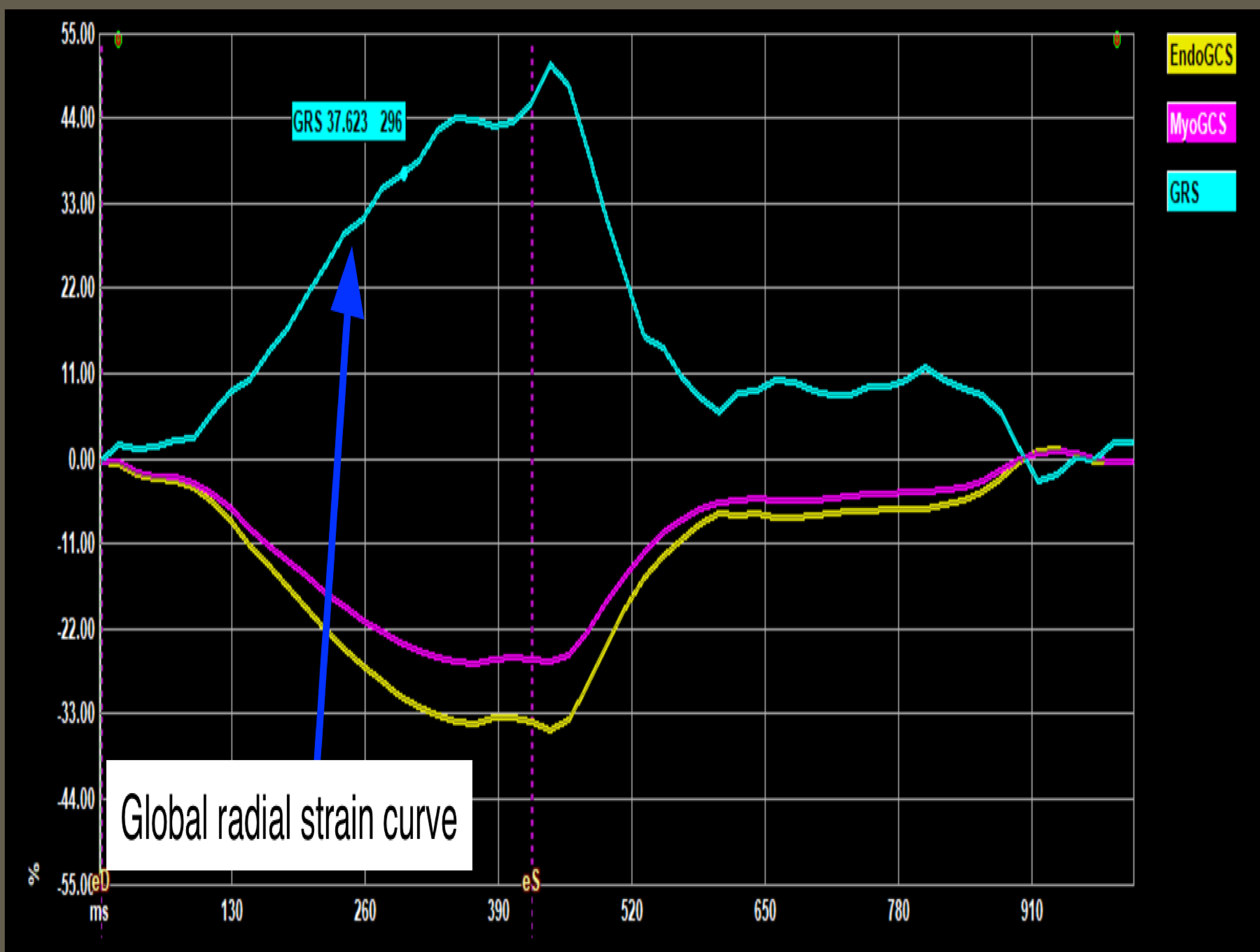

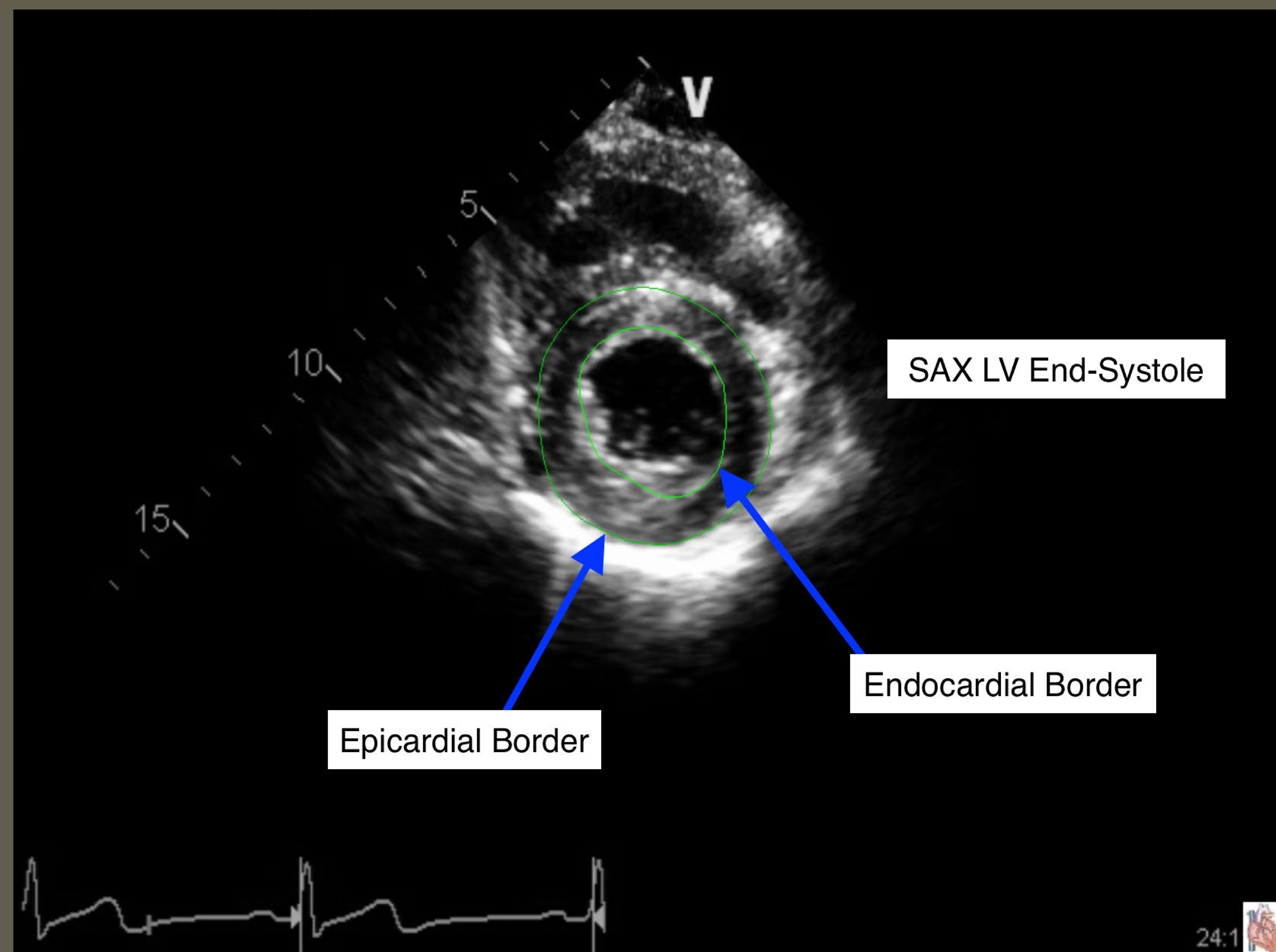

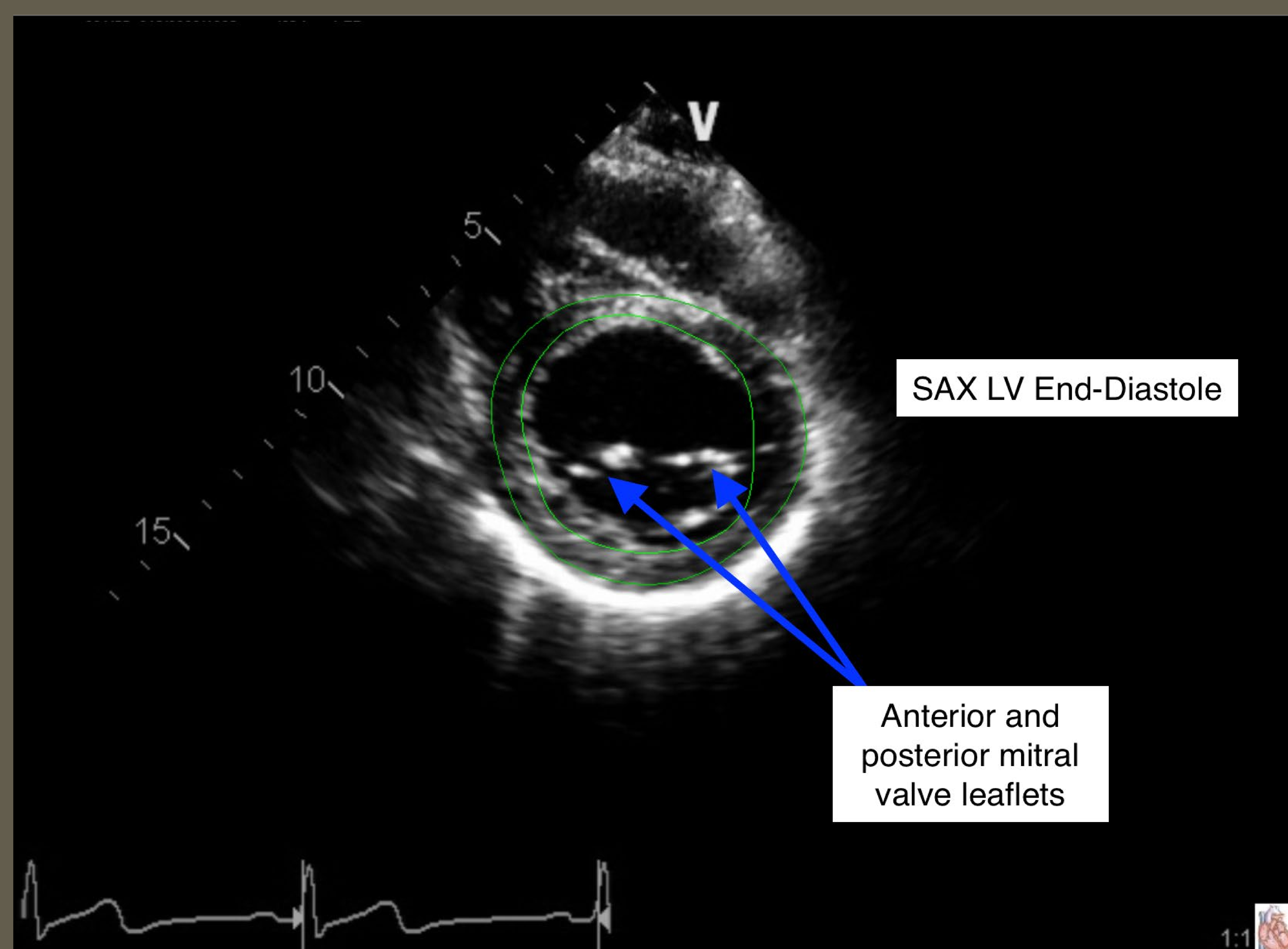

Figure 2. SAX Characterization of LV GRS or GCS function. The parasternal SAX views were similarly used to derive LV GRS or GCS strain curves as described in Fig 1. In the SAX image, the LV is traced in both end-systole (A) and end-diastole (B) at the level of the mitral valve (base). By tracking both epicardial and endocardial borders, strain curves (C) for GRS (%) versus time (ms) were generated. Each colored line represents the corresponding strain measurements derived from the SAX view.

Table 1. Inter and Intra-observer strain reliability statistical results

Inter-observer	Coefficient of Repeatability	Mean	Upper LoA	Lower LoA	ICC	CoV (%)
LVGLS	1.79 (95% CI 1.37-2.58)	0.1	1.9	-1.7	0.94	-4.27
LVGCS	7.68 (95% CI 5.88-11.09)	2.2	8.7	-4.4	0.87	-11.62
LVGRS	20.74 (95% CI 15.87-29.95)	-7.3	8.2	-22.7	0.79	20.99
LAGLS	32.50 (95% CI 24.86-46.93)	-8.1	21.1	-37.2	0.86	11.72
RAGLS	29.29 (95% CI 22.41-42.29)	9.6	32.6	-13.4	0.74	29.93
RVGLS	8.89 (95% CI 6.81-12.84)	2.3	10.2	-5.5	0.71	-19.14

Intra-observer 1	Observer 1 ICC	Observer 1 CoV (%)
LVGLS	0.93	-4.35
LVGCS	0.97	-4.26
LVGRS	0.93	11.1
LAGLS	0.97	9.97
RAGLS	0.92	11.16
RVGLS	0.78	-12.29

Intra-observer 2	Observer 2 ICC	Observer 2 CoV (%)
LVGLS	0.95	-4.46
LVGCS	0.98	-3.9
LVGRS	0.92	11.26
LAGLS	0.93	12.46
RAGLS	0.93	13.69
RVGLS	0.84	-15.78

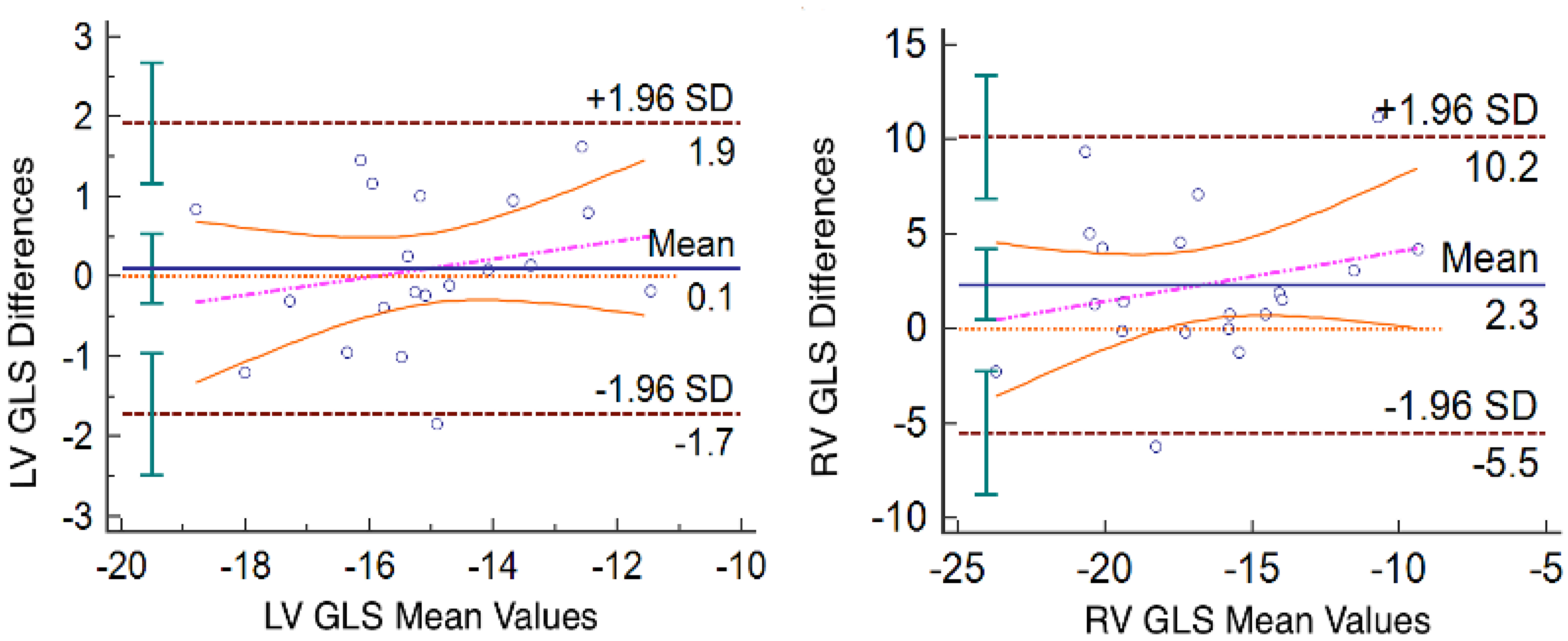

Figure 3. Bland-Altman plots for inter-observer strain measurements of LV GLS (left) and RV GLS (right). For LV GLS, the mean difference found between observers was 0.1 with the upper LoA at 1.9 and lower LoA at -1.7 (95% C.I. 1.37-2.58). For RV GLS, the mean difference found between observers was 2.3 with the upper LoA at 10.2 and lower LoA at -5.5 (95% C.I. 6.80-12.84). When comparing LV and RV GLS interobserver strain values, there is greater variability observed for RV GLS. Bland-Altman plots were additionally constructed for RV, RA, and LA chambers to display variability for GCS, GRS, and GLS. The relationship between image quality and interobserver differences was not statistically significant (p=0.82) but showed trend of higher variability with worse image quality. *LoA,* limits of agreement; *CI,* confidence interval.

Thank you for listening!